

The Arginine-Rich Hexapeptide R₄W₂ Is a Stereoselective Antagonist at the Vanilloid Receptor 1: A Ca²⁺ Imaging Study in Adult Rat Dorsal Root Ganglion Neurons

HERBERT M. HIMMEL,¹ THOMAS KISS, SEBESTYÉN J. BORVENDEG, CLEMENS GILLEN, and PETER ILLES

Rudolf-Boehm-Institut für Pharmakologie und Toxikologie, Medizinische Fakultät, Universität Leipzig, Leipzig (H.M.H., T.K., S.J.B., P.I.); and Abteilung Molekulare Pharmakologie, Grünenthal GmbH, Aachen (C.G.), Germany

Received December 26, 2001; accepted February 26, 2002 This article is available online at <http://jpet.aspetjournals.org>

ABSTRACT

Vanilloid receptors (VR) integrate various painful stimuli, e.g., noxious heat, acidic pH, capsaicin, and resiniferatoxin (RTX). Although VR antagonists may be useful analgesics, the available agents capsazepine and ruthenium red lack the necessary potency and selectivity. Recently, submicromolar concentrations of the arginine-rich hexapeptide RRRRWW-NH₂ (R₄W₂) blocked VR-mediated ionic currents in a *Xenopus* expression system in a noncompetitive and nonstereoselective manner. Here, VR-antagonistic effects of L-R₄W₂ and D-R₄W₂, hexapeptides consisting entirely of L- and D-amino acids, were characterized in native adult rat dorsal root ganglion neurons using [Ca²⁺]_i imaging (Fura-2/acetoxymethyl ester). Fura-2 fluorescence ratio (R) was increased by RTX and capsaicin by 0.473 ± 0.098 unit above basal levels of 0.903 ± 0.011 (R_{max}, 2.289 ± 0.031; R_{min}, 0.657 ± 0.007) in a concentration-dependent manner (log EC₅₀: RTX, -10.04 ± 0.05, n = 10; capsaicin, -6.60 ±

0.10, n = 11). Agonist concentration-response curves were shifted to the right by L- and D-R₄W₂ (0.1, 1, and 10 μM each) and by capsazepine (3, 10, 30, and 100 μM), whereas their maximal effects and slopes remained unaffected, indicating competitive antagonism. Schild analysis for L-R₄W₂ yielded apparent dissociation constants of 4.0 nM (RTX) and 3.7 nM (capsaicin), and slopes smaller than unity (RTX, 0.38; capsaicin, 0.42). Apparent dissociation constants and slopes for D-R₄W₂ and capsaicin were 153 nM and 0.67 versus 4.1 μM and 1.19 for capsazepine and capsaicin. Thus, VR-mediated effects in native dorsal root ganglion neurons were antagonized by L-R₄W₂ > D-R₄W₂ > capsazepine (order of potency). In conclusion, the R₄W₂ hexapeptide is a potent, stereospecific, and (probably) competitive VR antagonist, although an allosteric interaction cannot be completely ruled out.

Vanilloid receptors are activated by capsaicin, the pungent principle of chili pepper, resiniferatoxin (RTX) isolated from *Euphorbia resinifera*, and some other naturally occurring or synthesized compounds (for reviews see Holzer, 1991; Szallasi and Blumberg, 1999; Caterina and Julius, 2001). Since vanilloid receptors are located primarily on mammalian unmyelinated sensory C-fibers in dorsal root ganglia, their activation by tissue injury (nociception) ultimately leads to a conscious sensation of pain. Because the initial excitation of vanilloid receptors by agonists such as capsaicin or RTX is followed by long-lasting desensitization, these compounds are, despite their pungency, therapeutically used for the treatment of chronic pain states (Cruz et al., 1997; Hautkappe et al., 1998; Szallasi and Blumberg, 1999).

The recently cloned vanilloid receptor 1 (VR1; rat: Caterina

et al., 1997; human: Hayes et al., 2000) forms a Ca²⁺-permeable, nonselective cation channel that is currently believed to serve as an integrator of various painful stimuli such as capsaicin, RTX, noxious heat, acidic pH (Caterina et al., 1997; Tominaga et al., 1998; Caterina et al., 2000; Caterina and Julius, 2001; Greffrath et al., 2001; Savidge et al., 2001), and the endocannabinoid anandamide (Smart et al., 2000; Olah et al., 2001), particularly in inflamed tissue (Vyklícky et al., 1998). Furthermore, acidic conditions (Tominaga et al., 1998; McLatchie and Bevan, 2001), inflammatory mediators (bradykinin, serotonin, substance P: Vyklícky et al., 1998), cyclooxygenase and lipoxygenase products (prostaglandin E₂, Vyklícky et al., 1998; leukotriene B₄, 12-(S)-hydroperoxyeicosatetraenoic acid, Hwang et al., 2000), phosphorylation by protein kinases A and C (Premkumar and Ahern, 2000), and ATP-mediated activation of metabotropic P2Y-receptors (Tominaga et al., 2001) may act in unison to sensitize vanilloid receptors for noxious stimuli, thence lowering pain threshold and causing hyperalgesia (Davis et al., 2000).

Supported by the Bundesministerium für Bildung und Forschung: Leitprojekt "Molekulare Schmerzforschung" (01GG981/0).

¹ Present address: Dr. Herbert Himmel, Bayer AG, PH-PDT-CPSS, Safety Studies, Aprather Weg 18a, D-42096 Wuppertal, Germany.

ABBREVIATIONS: RTX, resiniferatoxin; VR, vanilloid receptor; [Ca²⁺]_i, cytosolic-free Ca²⁺ concentration; DRG, dorsal root ganglion; FITC, fluorescein isothiocyanate; HBSS, Hanks' balanced salt solution; ANOVA, analysis of variance; NMDA, N-methyl-D-aspartate.

However, only a few vanilloid receptor antagonists are available to date. Among them, capsazepine is a relatively weak competitive antagonist that has nonspecific effects at concentrations often required for antagonist activity, and ruthenium red is a weak and noncompetitive antagonist with a poorly defined mechanism of action (Bevan et al., 1992; Caterina et al., 1997; Docherty et al., 1997; Liu and Simon, 1997; Wardle et al., 1997; for reviews see Szallasi and Blumberg, 1999; Caterina and Julius, 2001). It was not until recently that three novel vanilloid receptor antagonists were described: the nonpungent capsaicin analog SDZ 249-665 (Urban et al., 2000), the highly potent compound iodo-RTX (Wahl et al., 2001), and the arginine-rich hexapeptide RRRRW-NH₂ (R₄W₂; Planells-Cases et al., 2000). Although the latter compound noncompetitively blocks recombinant VR1 channels expressed in *Xenopus* oocytes with submicromolar potency, its activity in native cells has yet to be ascertained. Here, we report that in primary cultures of adult rat dorsal root ganglion neurons, the arginine-rich hexapeptide R₄W₂ competitively antagonized the effects of capsaicin and RTX. The hexapeptide consisting entirely of L-amino acids, L-R₄W₂, was more potent than the respective stereoisomer D-R₄W₂.

Materials and Methods

Chemicals. Collagenase (type A, C-9891), 7S-nerve growth factor (N-0513), ITS-supplement (insulin-transferrin-selenium, I-3146), poly-L-lysine, trypan blue, ionomycin, digitonin, capsaicin, capsazepine, resiniferatoxin, and FITC-labeled *Bandeiraea simplicifolia* isolectin B₄ were obtained from Sigma Chemie (Deisenhofen, Germany). Dispase and DNase-1 were obtained from Roche Diagnostics (Mannheim, Germany) and Fura-2/acetoxymethyl ester from Molecular Probes (Eugene, OR). The D- and L-enantiomers of the arginine-rich hexapeptide R₄W₂ (sequence RRRRW-NH₂, purity >99.0% by high-performance liquid chromatography analysis) were gifts from Grünenthal (Aachen, Germany). All other chemicals were obtained at the highest available purity from Sigma or other commercial suppliers. Sterile disposable plastic ware for cell culture was by Falcon (BD Biosciences, Heidelberg, Germany), Nunc (Wiesbaden, Germany), or Nalgene (Nalge, Brussels, Belgium). Media, supplements, and trypsin for cell culture were obtained from Invitrogen (Eggenheim, Germany), and fetal bovine serum was obtained from Seromed (Berlin, Germany). Drugs were dissolved in water, methanol, or dimethyl sulfoxide and stored at -20°C. Aliquots of the stock solutions were diluted directly into the bath solution to achieve the final concentration. Solvents did not influence [Ca²⁺]_i measurements.

Isolation and Culture of Rat Dorsal Root Ganglion Cells. The present investigation was conducted in accordance with the principles outlined in the Declaration of Helsinki and the German law governing the Care and Use of Laboratory Animals, and was approved by the representative for animal care and use of the University of Leipzig. Adult rats (age 6–8 weeks) were killed by CO₂ and decapitation. Thoracic and abdominal organs were quickly removed, the spines were chilled at 4°C in Ca²⁺/Mg²⁺-free Hanks' balanced salt solution (HBSS), and thoracic and lumbar dorsal root ganglia were dissected and freed from connective tissue using fine tweezers and scissors under sterile conditions. Dorsal root ganglia collected in chilled HBSS were centrifuged (5 min, 124g) and resuspended in HBSS containing collagenase (0.5 mg/ml), dispase (1 mg/ml), and DNase-1 (1 mg/ml). After 40 to 50 min of incubation at 37°C in a shaking water bath, trypsin (0.6 mg/ml) was added for a further 15 min of incubation. After addition of medium 1 (Dulbecco's minimal essential medium, 35 mM total glucose, 2.5 mM L-glutamine, 15 mM

HEPES, 50 μg/ml gentamicin, 5% fetal bovine serum) to deactivate enzymes, the cell suspension was mechanically triturated using fire-polished Pasteur pipettes and passed through a cell strainer (mesh size 70 μm) to remove undigested tissue fragments. After centrifugation of the cell suspension (5 min at 194g), the pellet was resuspended in medium 1 supplemented with 30 ng/ml nerve growth factor, 10 μg/ml insulin, 5.5 μg/ml transferrin, and 5 ng/ml selenium. DRG cells were plated at a density of 2 × 10⁴ cells/ml onto poly(L-lysine)-coated (25 μg/ml) glass coverslips. Cultures were maintained for 2 to 4 days in a humidified atmosphere (37°C, 5% CO₂) before experimentation.

Intracellular Calcium Measurements. DRG cell cultures from days 2 to 4 were loaded for 50 to 60 min at 37°C in the dark with the cell permeant acetoxymethyl ester of the fluorescent Ca²⁺ indicator Fura-2 (1 μM). Simultaneously, cells were exposed to the FITC-labeled *Bandeiraea simplicifolia* isolectin IB₄ (0.1–0.5 μg/ml). To remove excess extracellular Fura-2 and IB₄, glass coverslips were washed several times with a modified Tyrode's solution (40.0 mM NaCl, 4.5 mM KCl, 2.0 mM CaCl₂, 1.0 mM MgCl₂, 10.0 mM HEPES, 10.0 mM glucose; pH adjusted to 7.4 with NaOH) and were allowed to rest for 30 min at room temperature protected from light. Thereafter, Ca²⁺ imaging experiments were performed at room temperature in Tyrode's solution using an inverted microscope (IX-70; Olympus, Hamburg, Germany) equipped for epifluorescence and a Peltier-cooled charge-coupled device camera (IMAGO; Till Photonic Inc., Martinsried, Germany). Intracellular Fura-2 was alternately excited at 340 nm and at 380 nm, and the emitted light was measured at a wavelength of 510 nm. The TILL visION software (release 3.3; Till Photonic Inc.) was used for data acquisition, system control, and, later, off-line data analysis.

Phase-contrast microphotographs taken at both the beginning and the end of an experiment served as documentation for the size (major and minor diameter averaged), integrity, and morphological nature of DRG cells. An ellipsoid-ovoid-spherical morphology was considered characteristic for neurons in contrast to the polygonal-flat-spindle-like shape of non-neuronal cells. In addition, a fluorescence image (excitation at 470 nm, emission at 510 nm) was recorded at the beginning of experiments for later quantification of FITC-IB₄ labeling of DRG cells. The fluorescence ratio (340 nm/380 nm) provides a relative measure of the cytosolic-free Ca²⁺ concentration ([Ca²⁺]_i; Grynkiewicz et al., 1985). The dynamic range of the observed fluorescence ratios was determined by measuring maximal and minimal fluorescence ratios, R_{max} and R_{min}. Sequential exposure of cells for 150 s each to a Tyrode's solution with high K⁺ (50 mM) containing 10 mM CaCl₂ and 10 μM ionomycin, and a nominally Ca²⁺-free Tyrode's solution containing 10 mM EGTA and 0.01% digitonin defined R_{max} and R_{min}, respectively. Averaging the results of several neurons, R_{max} amounted to 2.289 ± 0.031, and R_{min} was 0.657 ± 0.007 (n = 274). Because DRG neurons generally express high-voltage activated calcium channels (Petersen and LaMotte, 1991; Scroggs and Fox, 1992), only neurons tested for excitability and viability by depolarization with a high-KCl (50 mM) Tyrode's solution were included in the evaluation of data.

The experimental protocol routinely used started with the application of Tyrode's solution via the flush valve of a pressure-operated, computer-controlled rapid drug application device (DAD-12; NPI Electronic GmbH, Tamm, Germany), followed by high-K⁺ Tyrode's solution (94.5 mM NaCl, 50.0 mM KCl, 2.0 mM CaCl₂, 1.0 mM MgCl₂, 10.0 mM HEPES, 10.0 mM glucose; pH adjusted to 7.4 with NaOH) for 2 s. When the fluorescence ratio had returned to baseline after 3 min, a saturating concentration of ATP (500 μM) in nominally Ca²⁺-free Tyrode's solution supplemented with 0.5 mM EGTA was applied for 2 s as a test for metabotropic P2Y purinoceptors (data not shown; please see first gap in time axis in Fig. 1). Five minutes later, the vanilloid receptor agonists capsaicin and RTX were applied either alone or in the presence of antagonists such as capsazepine and R₄W₂ (antagonist exposure started 60 s before and lasted until 30 s after the agonist exposure). Since both capsaicin and RTX had a

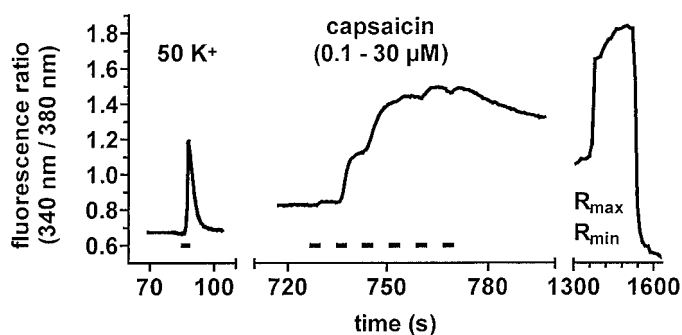


Fig. 1. Effect of vanilloid receptor agonist capsaicin on $[Ca^{2+}]_i$ in adult rat dorsal root ganglion neurons in primary culture. Time course of $[Ca^{2+}]_i$ was expressed as Fura-2 fluorescence ratio in a representative experiment. The neuron was depolarized by means of KCl (50 mM) and was exposed to capsaicin in concentrations of 0.1, 0.3, 1, 3, 10, and 30 μ M; the exposure time was 2 s each and is denoted by the dashes below the $[Ca^{2+}]_i$ trace. R_{max} and R_{min} were determined at the end of the experiment as defined under *Materials and Methods*.

rapid onset but a very slow decay of effect, the vanilloid receptor agonists were applied in a cumulative manner with an alternating 2 s of agonist exposure and a 6-s interval. The very slow decay of effect and the often incomplete return to baseline, even after extended periods of washout (10–15 min), restricted the application of capsaicin and RTX to the end of each experiment.

Statistical Analysis. Results were expressed as mean values \pm S.E.M. of n experiments if not indicated otherwise. Concentration-response curves were fitted to individual data sets using the following standard four-parameter logistic equation

$$\text{effect} = \text{min} + (\text{max} - \text{min}) / (1 + 10^{\exp(\log EC_{50} - \log [D]) \cdot n_H})$$

with minimal and maximal effect (min, max), half-maximal excitatory drug concentration (EC_{50}), drug concentration $[D]$, and Hill slope n_H . The minimal effect was treated as a constant ($= 0$) throughout, whereas the other parameters were variables. Statistical differences were analyzed by means of ANOVA followed by Dunnett's test versus the respective control group and considered significant at $p < 0.05$. If a nonparametric test was required, ANOVA on ranks followed by Dunn's test versus the control group was applied.

Results

In Fig. 1, the time course of $[Ca^{2+}]_i$, expressed as Fura-2 fluorescence ratio, is shown in a representative adult rat dorsal root ganglion neuron in primary culture. Elevating extracellular KCl concentration from 4.5 mM to 50 mM shifts the K^+ equilibrium potential from approximately -90 mV to about -29 mV (Nernst equation, $[K^+]_i = 155$ mM, room temperature). The ensuing depolarization of the neuron is associated with opening of voltage-dependent Ca^{2+} channels; the resulting $[Ca^{2+}]_i$ transient has a rapid onset, and elevated $[Ca^{2+}]_i$ returns to baseline level within seconds, demonstrating neuronal excitability and viability (Fig. 1). On average, KCl-induced depolarization increased the fluorescence ratio in neurons (as defined by their ellipsoid-ovoid-spherical shape) by 0.359 ± 0.013 over baseline levels of 0.862 ± 0.008 ($n = 397$, $p < 0.05$), whereas in non-neuronal cells (as defined by their polygonal-flat-spindle-like morphology), KCl-induced depolarization had a significantly smaller effect (ratio increase by 0.081 ± 0.016 , basal ratio 0.750 ± 0.019 , $n = 60$, $p < 0.05$). These results are consistent with the presence of voltage-gated Ca^{2+} channels in neurons and their near absence in the accompanying non-neuronal cells.

The experiment continued by exposing the neuron to in-

creasing concentrations of capsaicin (Fig. 1). Although rapid in onset, the VR-induced increase in $[Ca^{2+}]_i$ was sustained whether or not the agonists capsaicin (Fig. 1) or RTX (not shown) continued to be present, thus allowing the establishment of cumulative agonist concentration-response curves. The slow decline of agonist-induced elevated $[Ca^{2+}]_i$ levels toward baseline values is illustrated in the right part of Fig. 1. Even after prolonged washout (≥ 10 min) of either agonist, $[Ca^{2+}]_i$ signals remained elevated at approximately 50% of the maximum agonist effect as described before (Cholewinski et al., 1993). Both VR agonists, capsaicin and RTX, produced concentration-dependent increases in $[Ca^{2+}]_i$ at micromolar and nanomolar concentrations, respectively (Fig. 1, representative experiment; Fig. 2, average). Maximal increases in fluorescence ratio above baseline values were similar for capsaicin (0.511 ± 0.074 , $n = 145$) and for RTX (0.476 ± 0.080 , $n = 77$; not significant). Half-maximal effects were reached with 0.25 μ M capsaicin and with 0.091 nM RTX (compare Table 1 for complete list of parameters of concentration-response curves); these values are in line with published data (Jerman et al., 2000; McIntyre et al., 2001; for reviews see Szallasi and Blumberg, 1999; Caterina and Julius, 2001).

Concentration-response curves obtained with either VR agonist, capsaicin or RTX, were shifted to the right in the presence of the well characterized VR antagonist capsazepine (Table 1). The magnitude of this shift was significantly dependent on the concentration of capsazepine, whereas maximum effects of capsaicin and the Hill slopes of the respective concentration-response curves were not affected (Table 1), indicating a competitive antagonism of capsazepine at vanilloid receptors. Both RTX and capsaicin concentration-response curves were also shifted to the right by the arginine-rich hexapeptides L-R₄W₂ and D-R₄W₂ in a concentration-dependent manner (Table 1). The antagonist effect of L-R₄W₂ was already significant at 0.1 μ M, the lowest concentration tested, whereas the same concentration of D-R₄W₂ did not yet shift agonist concentration-response curves (Table 1;

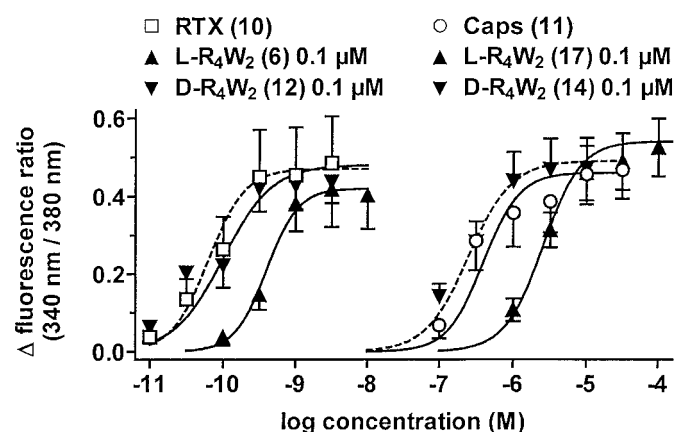


Fig. 2. Effect of vanilloid receptor agonists and antagonists on $[Ca^{2+}]_i$ in adult rat dorsal root ganglion neurons in primary culture. Concentration-response curves of resiniferatoxin (RTX)- and capsaicin (Caps)-induced increases in $[Ca^{2+}]_i$ under control conditions (RTX, \square ; Caps, \circ) and in the presence of 0.1 μ M arginine-rich hexapeptide L-R₄W₂ (\blacktriangle) and D-R₄W₂ (\blacktriangledown), respectively. Values are mean \pm S.E.M., and number of cells is given in parentheses. Curves were generated using the averages of parameters resulting from individual curve fittings. Mean values \pm S.E.M. for the curve parameters maximal effect, $\log EC_{50}$, and Hill slope are listed in Table 1.

TABLE 1

Parameters of concentration-response curves with the vanilloid receptor agonists capsaicin and RTX under control conditions and in the presence of the antagonists capsazepine (CZP), L-R₄W₂, and D-R₄W₂

Values are mean ± S.E.M. of *n* experiments; maximum is expressed as increase in Fura-2 fluorescence ratio (340 nm/380 nm) above baseline ratio. Statistical differences were analyzed by ANOVA, followed by Dunnett's multiple comparisons test versus control, with control being either capsaicin without antagonist or RTX without antagonist.

Agonist	Antagonist	<i>n</i>	Maximum	<i>p</i>	log EC ₅₀	<i>p</i>	Hill Slope	<i>p</i>
Capsaicin		11	0.466 ± 0.091		-6.60 ± 0.10		1.97 ± 0.21	
	CZP (3 μM)	19	0.463 ± 0.056	N.S.	-6.44 ± 0.05	N.S.	2.16 ± 0.18	N.S.
	CZP (10 μM)	12	0.429 ± 0.077	N.S.	-5.71 ± 0.08	*	1.59 ± 0.23	N.S.
	CZP (30 μM)	17	0.573 ± 0.042	N.S.	-5.53 ± 0.05	*	2.16 ± 0.27	N.S.
	CZP (100 μM)	11	0.429 ± 0.053	N.S.	-5.04 ± 0.21	*	1.50 ± 0.16	N.S.
	L-R ₄ W ₂ (0.1 μM)	14	0.523 ± 0.082	N.S.	-5.72 ± 0.09	*	1.72 ± 0.12	N.S.
	L-R ₄ W ₂ (1 μM)	14	0.527 ± 0.069	N.S.	-5.43 ± 0.07	*	1.54 ± 0.16	N.S.
	L-R ₄ W ₂ (10 μM)	11	0.470 ± 0.067	N.S.	-4.96 ± 0.15	*	1.86 ± 0.32	N.S.
	D-R ₄ W ₂ (0.1 μM)	14	0.489 ± 0.081	N.S.	-6.66 ± 0.07	N.S.	1.48 ± 0.11	N.S.
	D-R ₄ W ₂ (1 μM)	10	0.572 ± 0.098	N.S.	-5.73 ± 0.14	*	1.82 ± 0.19	N.S.
	D-R ₄ W ₂ (10 μM)	12	0.675 ± 0.100	N.S.	-5.23 ± 0.16	*	1.40 ± 0.15	N.S.
	RTX		10	0.481 ± 0.115		-10.04 ± 0.05		1.32 ± 0.23
CZP (10 μM)		7	0.517 ± 0.121		-9.64 ± 0.20		1.79 ± 0.27	
L-R ₄ W ₂ (0.1 μM)		6	0.420 ± 0.089	N.S.	-9.40 ± 0.06	*	1.99 ± 0.17	N.S.
L-R ₄ W ₂ (1 μM)		7	0.519 ± 0.081	N.S.	-9.09 ± 0.25	*	1.87 ± 0.41	N.S.
L-R ₄ W ₂ (10 μM)		13	0.446 ± 0.031	N.S.	-8.74 ± 0.13	*	1.68 ± 0.25	N.S.
D-R ₄ W ₂ (0.1 μM)		12	0.469 ± 0.069	N.S.	-10.21 ± 0.14	N.S.	1.75 ± 0.31	N.S.
D-R ₄ W ₂ (1 μM)		12	0.564 ± 0.081	N.S.	-9.55 ± 0.15	*	1.09 ± 0.14	N.S.
D-R ₄ W ₂ (10 μM)		10	0.389 ± 0.053	N.S.	-9.68 ± 0.06	N.S.	2.77 ± 0.43	*

* *p* < 0.05, statistically significant difference.

Fig. 2). This effect suggests a stereoselectivity of VR block by the hexapeptides, the L-enantiomer being a more potent antagonist than D-R₄W₂. Since neither the maximum agonist effects nor the Hill slopes of concentration-response curves were affected by either hexapeptide enantiomer, the mechanism of antagonist action of L-R₄W₂ and D-R₄W₂ may be a competitive one, too.

To characterize the mechanism of antagonist action of the hexapeptide enantiomers in more detail, a Schild analysis was performed, the results of which are depicted in Fig. 3. Because only one concentration-response curve could be established in each set of neurons due to the incomplete reversibility of agonist effects within reasonable times, concentration ratios for the Schild analysis were estimated based on the mean EC₅₀ values for the individual experimental groups listed in Table 1. The concentration ratio data so obtained were subject to linear regression analysis with the exception of D-R₄W₂ and RTX, where a linear relation between log(CR - 1) and antagonist concentration was apparently not obvious (Fig. 3A). Linear regression analysis of the data obtained with L-R₄W₂ and RTX or capsaicin yielded similar results. The apparent dissociation constants of L-R₄W₂ were

4.0 nM and 3.7 nM with RTX and capsaicin, respectively, as agonists. However, the regression lines were shallow, possessing slopes of 0.38 ± 0.01 (RTX) and 0.42 ± 0.04 (capsaicin) that were significantly smaller than unity (*p* < 0.05). With capsaicin as agonist, regression analysis yielded apparent antagonist dissociation constants of 153 nM for D-R₄W₂ and 4.1 μM for capsazepine, and slopes of 0.67 ± 0.06 (D-R₄W₂) and 1.19 ± 0.28 (capsazepine), which were significantly smaller than and indistinguishable from unity, respectively. Although these results support the notion of a stereoselectivity of block of vanilloid receptors by the hexapeptide enantiomers, with L-R₄W₂ being more potent than D-R₄W₂, they also suggest that the interaction between arginine-rich hexapeptides and the vanilloid receptor may not be as stoichiometric as that between capsazepine and VR.

Discussion

We have demonstrated for the first time in native rat dorsal root ganglion neurons, which are the most important peripheral integration site for noxious stimuli, that the positively charged arginine-rich hexapeptide R₄W₂ antagonizes vanilloid receptor-mediated effects in a stereoselective manner, with the peptide consisting of L-amino acids, L-R₄W₂, being more potent than D-R₄W₂. Both stereoisomers antagonized capsaicin- and RTX-induced [Ca²⁺]_i increases in an apparently competitive manner; however, the significant deviation from unity of Hill coefficients of concentration-response curves and of Schild plots is incompatible with the presence of a single binding site.

Thus, the present investigation confirms in native dorsal root ganglion neurons the potent (submicromolar) vanilloid receptor antagonist activity of the arginine-rich hexapeptide R₄W₂ that has been described recently in a *Xenopus* expression system (Planells-Cases et al., 2000), although the mechanism of antagonist action and its putative stereoselectivity are controversial. R₄W₂ blocked capsaicin-induced currents mediated by heterologously expressed VR1 channels in an apparently noncompetitive manner because of virtually iden-

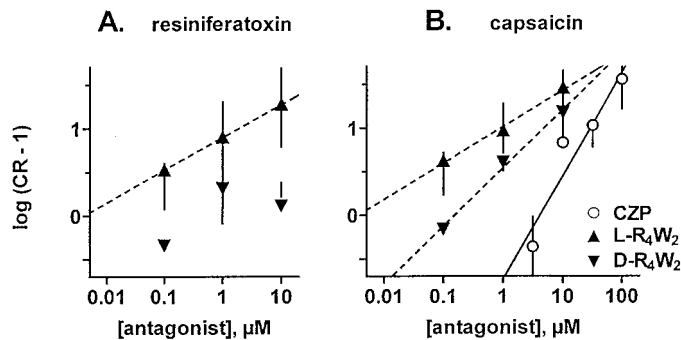


Fig. 3. Schild plots for L-R₄W₂ (▲), D-R₄W₂ (▼), and capsazepine (○) with resiniferatoxin (A) and capsaicin (B) as agonists. Note that mean values and ranges (min-max) are depicted. Apparent dissociation constants and respective slopes were estimated by means of linear regression analysis of the data.

tical capsaicin EC₅₀ concentrations in the absence and in the presence of the hexapeptide (Planells-Cases et al., 2000). In contrast, our results rather suggest the presence of a competitive antagonism since concentration-response curves for RTX and capsaicin were simply shifted along the concentration axis in the presence of R₄W₂ without maximum response or slope being affected (Fig. 2; Table 1).

Notwithstanding the possibility of more or less subtle differences in the properties of recombinant vanilloid receptors in a nonmammalian expression system versus native vanilloid receptor in DRG neurons in terms of VR1 homo-/hetero-oligomers, glycosylation state, or interacting modulatory proteins (Planells-Cases et al., 2000; Jahnke et al., 2001; Kedei et al., 2001), the present shift to the right of VR agonist concentration-response curves without a change in the maximum effect could not only be attributed to competitive antagonism (Clements and Westbrook, 1994), but might also reflect an allosteric interaction (Li et al., 1997, 1998). If R₄W₂ acted competitively at the capsaicin or RTX binding site, increasing hexapeptide concentrations would be expected to shift the agonist concentration-response curve to the right in a progressive and (almost) indefinite manner. Such a progressive shift was indeed observed with R₄W₂ concentrations over two orders of magnitude before limited drug supplies and elevated solvent concentrations precluded further experiments. If R₄W₂ acts at an allosteric site, the hexapeptide should cease to shift agonist concentration-response curves when its allosteric site(s) of action is(are) saturated; however, the corresponding curvilinear Schild plot reaching a limiting value at high concentrations of the antagonist R₄W₂ was not observed. Another method to discriminate between competitive and allosteric interaction relies on measuring activation and inactivation rates of vanilloid receptor channels, where a competitive antagonist will decrease the activation rate without changing the deactivation rate (Clements and Westbrook, 1994), whereas an increased deactivation rate and an unaffected activation rate are characteristic of an allosteric interaction (Li et al., 1997, 1998). However, this approach was unsuccessful since experimental conditions without desensitization of capsaicin-activated currents could not be satisfactorily established (data not shown).

Another putative explanation for the discrepancy between the results of Planells-Cases et al. (2000) and those of the present paper may become possible when considering the particular properties of cells (*Xenopus* expression system versus native rat dorsal root ganglion neurons) and signal detection methods used (voltage-clamp versus Ca²⁺ imaging). In the *Xenopus* expression system, the major, if not only, inward current (directly measured by means of the voltage-clamp technique) is mediated by recombinant vanilloid receptors, the block of which attenuates the maximal inward current flow, thus resembling a noncompetitive antagonism. Dorsal root ganglion neurons, on the other hand, possess a variety of ligand- and voltage-gated cation channels, and by means of Ca²⁺ imaging, the contribution from all participating Ca²⁺ sources (active Ca²⁺ conduits) is integrated. Na⁺ and Ca²⁺ influx via capsaicin- or RTX-activated vanilloid receptors is assumed to depolarize the neuron, thus serving as the trigger for opening of voltage-dependent Ca²⁺ channels. This is consistent with observations that VR-mediated [Ca²⁺]_i signals were depressed by removal of extracellular Na⁺ or by dihydropyridine block of voltage-dependent Ca²⁺

channels (data not shown; Greffrath et al., 2001). Since a very small inward current of only a few picoamperes may suffice as trigger for a large depolarization and the ensuing full-size Ca²⁺ influx, the maximal signal detected by Ca²⁺ imaging may be preserved even when the trigger, i.e., the cation current via vanilloid receptor channels, is markedly reduced, thus resembling a competitive antagonism.

In terms of a putative stereoselective mechanism of action, it has been reported that equal concentrations of L-R₄W₂ and D-R₄W₂, blocked heterologously expressed VR1 channels with similar efficacy, suggesting lack of stereoselectivity of block, whereas only the D-hexapeptide significantly decreased capsaicin-induced ocular irritation in mice, seemingly because it is proteolysis-resistant (Planells-Cases et al., 2000). In contrast, the present results clearly support the conclusion of a stereoselective antagonism with L-R₄W₂ being more potent than D-R₄W₂ (Fig. 2; Table 1). Membrane-bound extracellularly oriented peptidases acting on a broad range of substrates occur throughout the nervous system in and ex vivo (Konkoy and Davis, 1996) and also in mixed neuronal/glia cell cultures from dorsal root ganglia (Berger et al., 1995). However, an ostensible stereoselectivity due to preferential proteolytic degradation of one of the hexapeptide enantiomers is discounted, because the "physiological" L-R₄W₂ is expected to be more susceptible to proteolysis than D-R₄W₂, whereas the latter was clearly less potent than the former.

Furthermore, Hill coefficients around unity are consistent with the occurrence of a single binding site in heterologously expressed vanilloid receptors (Planells-Cases et al., 2000), whereas in rat dorsal root ganglion neurons the results from Schild analysis are incompatible with a single binding site, suggesting, instead, the presence of several binding sites (Fig. 3). One of these several putative binding sites is most likely located on the pore loop of the vanilloid receptor, because the amino acid sequence of the pore loop contains four negatively charged residues (E636, D646, E648, and E651) that may constitute a binding site for positively charged molecules. Although this very binding site apparently does not discriminate between L-R₄W₂ and D-R₄W₂ (Planells-Cases et al., 2000), other arginine-rich hexapeptide binding sites do so, e.g., *N*-methyl-D-aspartate (NMDA) receptors where D-R₄W₂ has been reported to be twice as potent as L-R₄W₂ (Ferrer-Montiel et al., 1998). Thus, one might speculate that the large number of NMDA receptors present in rat dorsal root ganglion neurons preferentially bind D-R₄W₂, thus acting as a sink for the D-hexapeptide, thereby resulting in the observed apparent stereoselective antagonism at vanilloid receptors.

In conclusion, both synthetic (e.g., R₄W₂) and naturally occurring (e.g., dynorphin A) arginine-rich hexapeptides have been demonstrated to possess antagonist activity at NMDA and vanilloid receptors (Ferrer-Montiel et al., 1998; Planells-Cases et al., 2000; present paper), which constitute important sites within the pain pathway for integration of noxious stimuli. The present data are consistent with R₄W₂ acting as a stereoselective and competitive antagonist at native vanilloid receptors in dorsal root ganglion neurons, although an allosteric interaction cannot be totally excluded. Future work will show whether it will be possible to develop a low molecular weight molecule that mimics the antagonist action of arginine-rich hexapeptides at NMDA and vanilloid

receptors and may prove a useful analgesic for the treatment of chronic pain.

Acknowledgments

We thank Helga Sobottka for expert technical assistance with cell isolation and culture.

References

- Berger UV, Carter RE, McKee M, and Coyle JT (1995) N-acetylated alpha-linked acidic dipeptidase is expressed by non-myelinating Schwann cells in the peripheral nervous system. *J Neurocytol* **24**:99–109.
- Bevan S, Hothi S, Hughes G, James IF, Rang HP, Shah K, Walpole CSJ, and Yeats J (1992) Capsazepine—a competitive antagonist of the sensory neurone excitant capsaicin. *Br J Pharmacol* **107**:544–552.
- Caterina MJ and Julius D (2001) The vanilloid receptor: a molecular gateway to the pain pathway. *Annu Rev Neurosci* **24**:487–517.
- Caterina MJ, Leffler A, Malmberg AB, Martin WJ, Trafton J, Peterson-Zeitl KR, Klotzberg M, Basbaum AI, and Julius D (2000) Impaired nociception and pain in mice lacking the capsaicin receptor. *Science (Wash DC)* **288**:306–313.
- Caterina MJ, Schumacher MA, Tominaga M, Rosen TA, Levine JD, and Julius D (1997) The capsaicin receptor: a heat-activated ion channel in the pain pathway. *Nature (Lond)* **389**:816–824.
- Cholewinski A, Burgess GM, and Bevan S (1993) The role of calcium in capsaicin-induced desensitization in rat cultured dorsal root ganglion neurons. *Neuroscience* **55**:1015–1023.
- Clements JD and Westbrook GL (1994) Kinetics of AP5 dissociation from NMDA receptors: evidence for two identical cooperative binding sites. *J Neurophysiol* **71**:2566–2569.
- Cruz F, Guimaraes M, Silva C, and Reis M (1997) Suppression of bladder hyperreflexia by intravesical resiniferatoxin. *Lancet* **350**:640–641.
- Davis JB, Gray J, Gunthorpe MJ, Hatcher JP, Davey PT, Overend P, Harries MH, Latcham J, Clapham C, Atkinson K, et al. (2000) Vanilloid receptor-1 is essential for inflammatory thermal hyperalgesia. *Nature (Lond)* **405**:183–187.
- Docherty RJ, Yeats JC, and Piper AS (1997) Capsazepine block of voltage-activated calcium channels in adult rat dorsal root ganglion neurones in culture. *Br J Pharmacol* **121**:1461–1467.
- Ferrer-Montiel A, Merino JM, Blondelle SE, Perez-Paya E, Houghten RA, and Montal M (1998) Selected peptides targeted to the NMDA receptor channel protect neurons from excitotoxic death. *Nat Biotechnol* **16**:286–291.
- Greffrath W, Kirschstein T, Nawrath H, and Treede RD (2001) Changes in cytosolic calcium in response to noxious heat and their relationship to vanilloid receptors in rat dorsal root ganglion neurons. *Neuroscience* **104**:539–550.
- Gryniewicz G, Poenie M, and Tsien RY (1985) A new generation of Ca²⁺ indicators with greatly improved fluorescence properties. *J Biol Chem* **260**:3440–3450.
- Hautkappe M, Roizen MF, Toledano A, Roth S, Jeffries JA, and Ostermeier AM (1998) Review of the effectiveness of capsaicin for painful cutaneous disorders and neural dysfunction. *Clin J Pain* **14**:97–106.
- Hayes P, Meadows HJ, Gunthorpe MJ, Harries MH, Duckworth DM, Cairns W, Harrison DC, Clarke CE, Ellington K, Prinjha RK, et al. (2000) Cloning and functional expression of a human orthologue of rat vanilloid receptor 1. *Pain* **88**:205–215.
- Holzer P (1991) Capsaicin: cellular targets, mechanisms of action and selectivity for thin sensory neurons. *Pharmacol Rev* **43**:143–201.
- Hwang SW, Cho H, Kwak J, Lee SY, Kang CJ, Jung J, Cho S, Min KH, Suh YG, Kim D, and Oh U (2000) Direct activation of capsaicin receptors by products of lipoxygenases: endogenous capsaicin-like substances. *Proc Natl Acad Sci USA* **97**:6155–6160.
- Jahnel R, Dreger M, Gillen C, Bender O, Kurreck J, and Hucho F (2001) Biochemical characterization of the vanilloid receptor 1 expressed in a dorsal root ganglia derived cell line. *Eur J Biochem* **268**:5489–5496.
- Jerman JC, Brough SJ, Prinjha R, Harries MH, Davis JB, and Smart D (2000) Characterization using FLIPR of rat vanilloid receptor (rVR1) pharmacology. *Br J Pharmacol* **130**:916–922.
- Kedei N, Szabo T, Lile JD, Treanor JJ, Olah Z, Iadarola MJ, and Blumberg PM (2001) Analysis of the native quaternary structure of vanilloid receptor 1. *J Biol Chem* **276**:28613–28619.
- Konkoy CS and Davis TP (1996) Ectoenzymes as sites of peptide regulation. *Trends Pharmacol Sci* **17**:288–294.
- Li CY, Peoples RW, and Weight FF (1997) Mg²⁺ inhibition of ATP-activated current in rat nodose ganglion neurons: evidence that Mg²⁺ decreases the agonist affinity of the receptor. *J Neurophysiol* **77**:3391–3395.
- Li CY, Peoples RW, and Weight FF (1998) Ethanol-induced inhibition of a neuronal P2X purinoceptor by an allosteric mechanism. *Br J Pharmacol* **123**:1–3.
- Liu L and Simon SA (1997) Capsazepine, a vanilloid receptor antagonist, inhibits nicotinic acetylcholine receptors in rat trigeminal ganglia. *Neurosci Lett* **228**:29–32.
- McIntyre P, McLatchie LM, Chambers A, Phillips E, Clarke M, Savidge J, Toms C, Peacock M, Shah K, Winter J, et al. (2001) Pharmacological differences between the human and rat vanilloid receptor 1 (VR1). *Br J Pharmacol* **132**:1084–1094.
- McLatchie LM and Bevan S (2001) The effects of pH on the interaction between capsaicin and the vanilloid receptor in rat dorsal root ganglia neurons. *Br J Pharmacol* **132**:899–908.
- Olah Z, Karai L, and Iadarola MJ (2001) Anandamide activates vanilloid receptor 1 at acidic pH in DRG neurons and cells ectopically expressing VR1. *J Biol Chem* **276**:31163–31170.
- Petersen M and LaMotte RH (1991) Relationship between capsaicin sensitivity of mammalian sensory neurons, cell size and type of voltage-gated Ca currents. *Brain Res* **561**:20–26.
- Planells-Cases R, Aracil A, Merino JM, Gallar J, Perez-Paya E, Belmonte C, Gonzalez-Ros JM, and Ferrer-Montiel AV (2000) Arginine-rich peptides are blockers of VR-1 channels with analgesic activity. *FEBS Lett* **481**:131–136.
- Premkumar LS and Ahern GP (2000) Induction of vanilloid receptor channel activity by protein kinase C. *Nature (Lond)* **408**:985–990.
- Savidge JR, Ranasinghe SP, and Rang HP (2001) Comparison of intracellular calcium signals evoked by heat and capsaicin in cultured rat dorsal root ganglion neurons and in a cell line expressing the rat vanilloid receptor VR1. *Neuroscience* **102**:177–184.
- Scroggs RS and Fox AP (1992) Calcium current variation between acutely isolated adult rat dorsal root ganglion neurons of different size. *J Physiol (London)* **445**:639–658.
- Smart D, Gunthorpe MJ, Jerman JC, Nasir S, Gray J, Muir AI, Chambers JK, Randall AD, and Davis JB (2000) The endogenous lipid anandamide is a full agonist at the human vanilloid receptor (hVR1). *Br J Pharmacol* **129**:227–230.
- Szallasi A and Blumberg PM (1999) Vanilloid (capsaicin) receptors and mechanisms. *Pharmacol Rev* **51**:159–211.
- Tominaga M, Caterina MJ, Malmberg AB, Rosen TA, Gilbert H, Skinner K, Raumann BE, Basbaum AI, and Julius D (1998) The cloned capsaicin receptor integrates multiple pain-producing pathways. *Neuron* **21**:531–543.
- Tominaga M, Wada M, and Masu M (2001) Potentiation of capsaicin receptor activity by metabotropic ATP receptors as a possible mechanism for ATP-evoked pain and hyperalgesia. *Proc Natl Acad Sci USA* **98**:6951–6956.
- Urban L, Campbell EA, Panesar M, Patel S, Chaudhry N, Kane S, Buchheit KH, Sandells B, and James IF (2000) In vivo pharmacology of SDZ 249–665, a novel non-pungent capsaicin analogue. *Pain* **89**:65–74.
- Vyklicky L, Knotkova-Urbancova H, Vitaskova Z, Vlachova V, Kress M, and Reeh PW (1998) Inflammatory mediators at acidic pH activate capsaicin receptors in cultured sensory neurons from newborn rats. *J Neurophysiol* **79**:670–676.
- Wahl P, Foged C, Tullin S, and Thomsen C (2001) Iodo-resiniferatoxin, a new potent vanilloid receptor antagonist. *Mol Pharmacol* **59**:9–15.
- Wardle KA, Ranson J, and Sanger GJ (1997) Pharmacological characterization of the vanilloid receptor in the rat dorsal spinal cord. *Br J Pharmacol* **121**:1012–1016.

Address correspondence to: Dr. Herbert Himmel, Bayer AG, PH-PDT-CPSS, Safety Studies, Aprather Weg 18a, D-42096 Wuppertal, Germany. E-mail: herbert.himmel.hh@bayer-ag.de